CrossMark

The recyclable cotton cellulose nanofibers/ZnO/CuS nanocomposites with enhanced visible light photocatalytic activity

Xiufang Zhang[1] · Jie Mei[2] · Song Wang[1] · Yingying Zheng[1] · Can Cui[1] · Jiaqi Pan[1] · Chaorong Li[1]

Abstract The cotton cellulose nanofibers(CCNFs)/ZnO/CuS nanocomposites have been successfully fabricated by the electrospun-hydrothermal method and successive ionic layer adsorption. The results of XRD, SEM and TEM indicate that the CuS are successfully combined with the ZnO. The photocatalytic activity of the CCNFs/ZnO/CuS nanocomposites is investigated by the degradation of methylene blue under visible light irradiation, and it is demonstrated to be significantly enhanced after the CuS is introduced. Furthermore, the direct interfacial charge transfer of the ZnO/CuS is considered as the main reason for the enhancement.

1 Introduction

Cotton cellulose, as an abundant polymer in nature, with vast attractive properties, including biocompatibility, biodegradability, thermal and chemical stability [1]. Particularly, it can be processed into various forms, such as membrane, sponges, microspheres, non-woven or knitted

✉ Jiaqi Pan
panjq@zstu.edu.cn

1 Department of Physics, and Key Laboratory of ATMMT Ministry of Education, Zhejiang Sci-Tech University, Hangzhou 310018, People's Republic of China

2 School of Chemistry & Bioengineering, Taizhou College of Nanjing Normal University, Taizhou 225300, People's Republic of China

textiles, which promote it for being widely used in the industry. With the further research, the applications of the cotton cellulose is vastly expanded, especially incorporation of various functional nanomaterials into cotton cellulose, which is regarded as one of the most effective ways for improving the surface properties of nanomaterials. Unquestionable, the interfacial bonding force between cotton fibers and nanometer material is the most important factor to form functionalized cotton fiber. Compared with the microfibers, the nanofibers with higher surface volume value and smaller diameter [2, 3] could provide large numbers of favorable coordination active sites, which may introduce lots of remarkable physical and chemical properties and makes them to be a competitive candidate in many important applications, such as thin-film transistors, lithium-ion batteries or tissue scaffolds [4–7], including the photocatalytic pollutant degradation, and our previous work have also researched about the electrospinning method to obtain ultra-fine natural cotton cellulose nanofibers [8].

With the rapid development of industry, the increasingly environmental pollution has attracted researchers' extensive attention. Series of ways are explored to ease the actuality, including the physical and chemical method, especially the photocatalysis, with the low cost and high recycle, is considered as a green and continuable ways. Up to now, lots of researches have been done, such as ZnO nanoparticles [9], nanosheets, TiO_2 nanotubes [10], and so on. However, most of the photocatalysts could acquire further improving with the good dispersibility. What's more, in view of the economic efficiency, the recycling of the photocatalyst is another important factor in future application.

Based on above reasons, the cotton nanofibers is chose as an ideal substrate to load and disperse the photocatalysts

with its recoverable toughness fibrous structure and sufficient load sites. Compared with other materials, ZnO nanomaterials have been studied extensively due to their high controllability, physical and chemical stability [11–13]. However, limited by its wide bandgap (3.37 eV), a drawback of using in photocatalysis is that it could be only activated by UV light. As the typical method, the metal/semiconductor or semiconductor heterojunction materials provide a novel ideal to ameliorate the actuality, because those structures could increase the light absorption and utilization, modify band gap position, facilitate charge rectification and improve carrier separation efficiently. Series of metal modified photocatalyst have been researched and acquired encouraging results, such as Pt [14, 15], Au [16, 17] and Ag [18], which display an obvious enhancement. On the other hand, in view of costing, narrow band gap materials modified semiconductor heterojunctions with the increasing visible light absorption and high-efficiency carrier separation play an important role in photocatalysis, such as CdSe/ZnO [19], CdS/ZnO [20] or PbS/ZnO [21]. However, the toxicity and harmful effects of cadmium or plumbum couldn't be neglected. Hence, various environmentally friendly materials have been investigated, in particular the CuS, as an eco-friendly and economic materials has become a research focus in visible light photocatalysis [22–26].

In this paper, we prepared the CCNFS/ZnO/CuS composites with excellent visible light photocatalyst by a simple electrospun-hydrothermal method and successive ionic layer adsorption reaction. Further, the mechanism of enhancement of visible light photocatalytic activity was investigated.

2 Experimental

2.1 Chemicals and materials

Cotton cellulose (DP = 12,000) got from Zhejiang Academy of Agricultural Sciences. Methanol (CH_3OH, C99.5%, AR), anhydrous ethanol (C_2H_5OH, C99.7%, AR) were purchased from Hangzhou GaoJing Chemical Reagent Co. Ltd. The N, N-dimethylacetamide(DMAc, C99.5%, AR), hexamethylene tetramine(HMTA, C99.0%, AR), zinc nitrate($Zn(NO_3)_2 \cdot 6H_2O$, C99.0%, AR), zinc acetate($Zn(CH_3COO)_2 \cdot 2H_2O$, C99.0%, AR) were supplied by Tianjin YongDa Chemical Reagent Development Center. Lithium chloride(LiCl, C99.5%, AR), coppeer acetate monohydrate ($CuCOOH \cdot H_2O$, C99.95%, AR), sodium sulfide nonahydrate($Na_2S \cdot 9H_2O$, C98.0%, AR) were purchased from Aladdin Reagent Co. Ltd., sodium sulfide nonahydrate($Na_2S \cdot 9H_2O$, C98.0%, AR) were purchased from Shanghai Macklin Biochemical Co. Ltd. The

cotton cellulose and chemicals were used without further purification, LiCl was preprocessed to remove the water.

2.2 Preparation of CCNFs/ZnO/CuS nanocomposites

CCNFs were obtained by electrospinning process according to our previous work [8]. The growth of ZnO nanorod has been achieved by hydrothermal synthetic method. Firstly, the cotton nanofibers were drop-coated 15 times with 20 mM zinc acetate($Zn(CH_3COO)_2 \cdot 2H_2O$) ethanol solution and annealed at 150 °C for 3 h to get the ZnO seed layer. Then, the CCNFs with ZnO seed layer was placed in a 30 ml autoclave containing an aqueous solution of 25mMol $Zn(NO_3)_2 \cdot 6H_2O$ and 25 mMol HMTA. The autoclave was sealed in an electric oven under 90 °C for 10 h. Finally, CuS nanoparticles were deposited on CCNFs/ZnO by the successive ionic layer adsorption reaction [15]. The as-prepared CCNFs/ZnO were immersed in 50 mMol $Na_2S \cdot 9H_2O$ and keep 5 min, then immersed in 25 mMol $CuCOOH \cdot H_2O$ for 5 min. Such a cycle was repeated 2×0, 2×1, 2×2, 2×3 times and the obtained samples were labeled as C–Zn–Cu-0, C–Zn–Cu-1, C–Zn–Cu-2, C–Zn–Cu-3, respectively. Between two processing cycles, the sheets were kept drying for 5 min at 50 °C.

2.3 Characterization methods

The surface morphology and structure of the samples were investigated using Field-emission scanning electron microscope (FESEM, Hitachi S-4800). The crystal structures of the samples were further characterized by X-ray diffraction (XRD, Bruker AXS D8-discover, Cu-Ka of 1.5418A) and transmission electron microscope (TEM, JEM-2100, 200 kV). UV–Vis absorption spectrophotometer (U-3900 Hitachi equipped with a 30 mm integrating sphere) was used to investigate ultraviolet and photocatalytic performance of the nanocomposites.

2.4 Photocatalytic activity

The photocatalytic activities of the synthesized samples were evaluated by the photocatalytic degradation of MB in an aqueous solution under visible irradiation (PHILIPS, 500 W, $\lambda \geq 420$ nm). In the experiment, 50 mg of photocatalyst were added into 60 mL MB solution (10 mg/L). Prior to irradiation, the solution mixture was agitated for 30 min to ensure the adsorption–desorption equilibrium. The catalyst suspension was subsequently irradiated under visible light. Adequate aliquots (4 mL) of the suspension were extracted for analysis. The filtrates were analyzed by recording variations at the wavelength of maximal

absorption in the UV–Vis spectrophotometer. Where C_0 was the absorbance of solution in adsorption–desorption equilibrium, while C was the absorbance of solution in different duration.

3 Results and discussion

Figure 1 is the XRD spectra of the as-prepared CCNFs/ZnO/CuS with different ratio. As shown, the noncrystalline CCNFs without obvious diffraction peak, including the C–Zn-Seed, which could be attributed that the ZnO seeds with low crystallinity and the less concentration. As revealed, the C–Zn–Cu-0 shows typical diffraction peaks of ZnO(PDF-36-1451), which is corresponding to previously literatures [9]. With the cycle time increasing, the peaks of CuS(JCPDS-no. 06-0464) enhanced gradually, which could be ascribed to the increasing amount and crystallinity of the CuS, but some peaks of pure CuS didn't exist in the nanocomposites, which indicate that the nanoparticles own the preferential growth [27]. It's interesting that the (103) peak of CuS superpose with the (100) peak of ZnO, as shown, about the 31.8°, the intensity of the peak increase with the CuS and exhibits an obviously broadened, which could be attributed to the smaller grain size of the CuS. All above indicate that the CCNFs/ZnO/CuS nanocomposites are successfully prepared.

Figure 2 shows the morphology of the samples in different stage. Figure 2a is the SEM of the as-prepared pure CCNFs, as seen that the interlaced CCNFs with a diameter of about 100–200 nm is uniform and smooth, which could provide sufficient site for ZnO seeds. As shown in Fig. 2b, compared with the pure CCNFs, after the ZnO seeds are coated onto the surface, the fibers become rough. With the further crystal growth, Fig. 1c is the CCNFs/ZnO
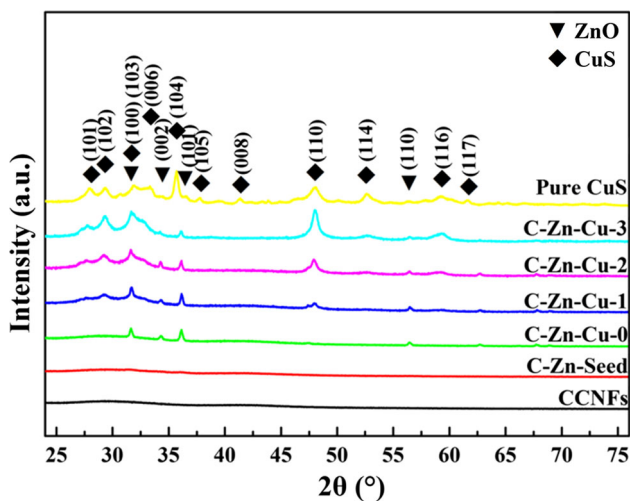
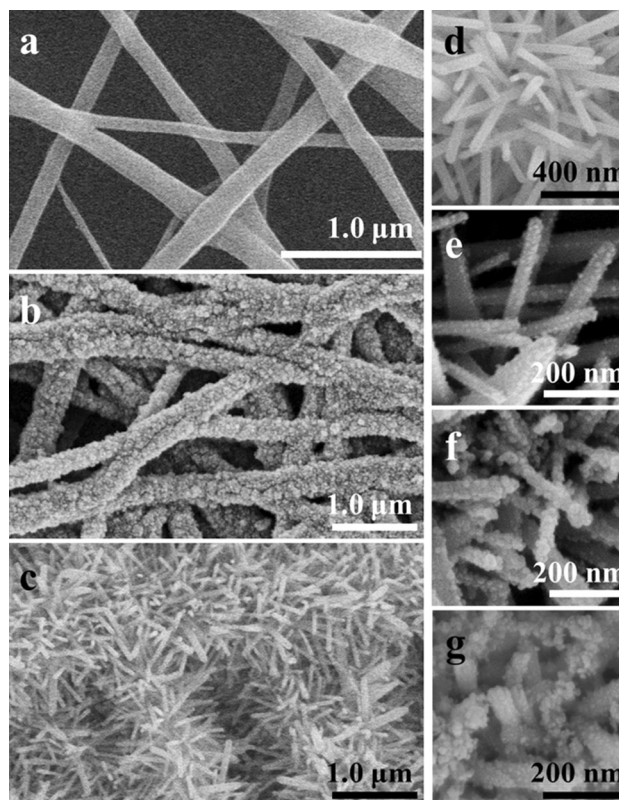Fig. 1 The XRD spectra of the CCNFs/ZnO/CuS with different ratio

Fig. 2 SEM of the CCNFs/ZnO/CuS. **a** the as-prepared CCNFs, **b** the CCNFs/ZnO Seeds, **c** the CCNFs/ZnO, **d–g** high resolution SEM images of C–Zn–Cu-0, C–Zn–Cu-1, C–Zn–Cu-2, C–Zn–Cu-3

nanorods, which clearly shows that the ZnO nanorods tightly cover the surface of the CCNFs. Figure 2d–g show the high resolution SEM images of CCNFs/ZnO with different concentration of CuS(C–Zn–Cu-0, C–Zn–Cu-1, C–Zn–Cu-2, C–Zn–Cu-3). As shown in Fig. 2d, the as-prepare CCNFs/ZnO without deposited CuS is smoothly and with uniform diameter about 60–80 nm, lengths about 600–800 nm. As shown in Fig. 2e–f, the ZnO branches become rough and the nanoparticles increase with the cycling times during synthesis obviously, those could be attributed to that the CuS deposited on the surface of the ZnO nanorods. It is evident that the grain size and the distribution of CuS nanoparticles are homogeneous, and the further structures are characterized by TEM.

Figure 3a is the TEM of the C–Zn–Cu-2. As shown, the rodlike ZnO branch is covered with CuS nanoparticles, which is corresponding to the SEM images. Further, the HRTEM is used to characterize the crystal structure. As shown in Fig. 3b and c, the lattice spacing of 0.247 nm corresponds to the (101) plane of the ZnO and the lattice spacing of 0.321 nm corresponds to the (101) plane of the CuS, respectively (The TEM images of C–Zn–Cu-0, C–Zn–Cu-1, C–Zn–Cu-2, C–Zn–Cu-3 are shown in ESI Fig. S1).
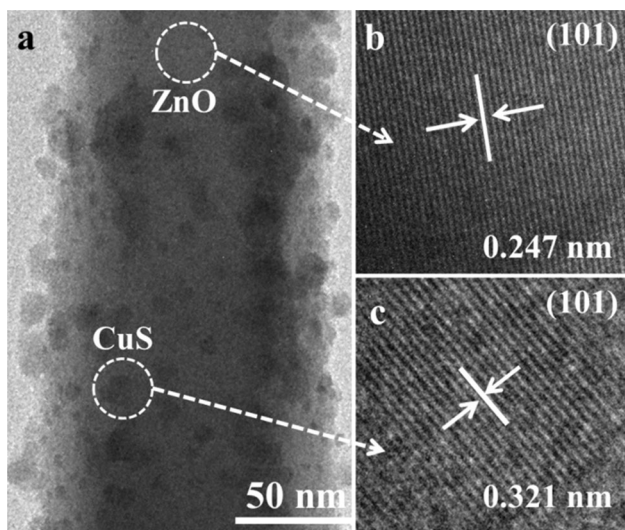
Fig. 3 TEM of the CCNFs/ZnO/CuS. **a** TEM of the single CCNFs/ZnO/CuS nanocomposites, **b** HRTEM of ZnO, **c** HRTEM of CuS

Figure 4 is the XPS of the as-prepared CCNFs/ZnO/CuS nanocomposites. As shown in Fig. 4a, the full survey indicate that the presence of Zn, Cu, S in the as-prepared

sample. In Fig. 4b the two peaks fitted at 1021.5 1044.7 eV correspond to the Zn 2p 3/2 and Zn 2p 1/2 of ZnO, respectively. Two strong peaks at 935.1 and 955.1 eV are observed in the Fig. 4c, consistent with the reported values of binding energies of Cu^{2+} 2p3/2 and 2p1/2, respectively. It's interesting that, on the sides of Cu^{2+} 2p3/2 and 2p1/2, two high-intensity components (932.2 and 952.1 eV) appeared, which could be assigned to the Cu^+ oxidation state, which is corresponded to the previous literature [28]. In addition, the satellite peaks further confirms the existence of Cu^{2+} vacancy [28]. In Fig. 4d, the main peak at 162.7 eV is attributed to S 2p.

The result of the XRD measurement, together with the result of the SEM, HRTEM and XPS measurement suggest that the CuS nanoparticles are successfully introduced into the CCNFs/ZnO system.

As shown in Fig. 5, the as-prepared CCNFs/ZnO(C–Zn–Cu-0) exhibits weak absorption in the visible region of 400–800 nm, while all the CCNFs/ZnO/CuS composites exhibit obvious absorption in visible region, as the curves shown, the absorption intensity increases with the amount of CuS, which is corresponded to previous literatures and
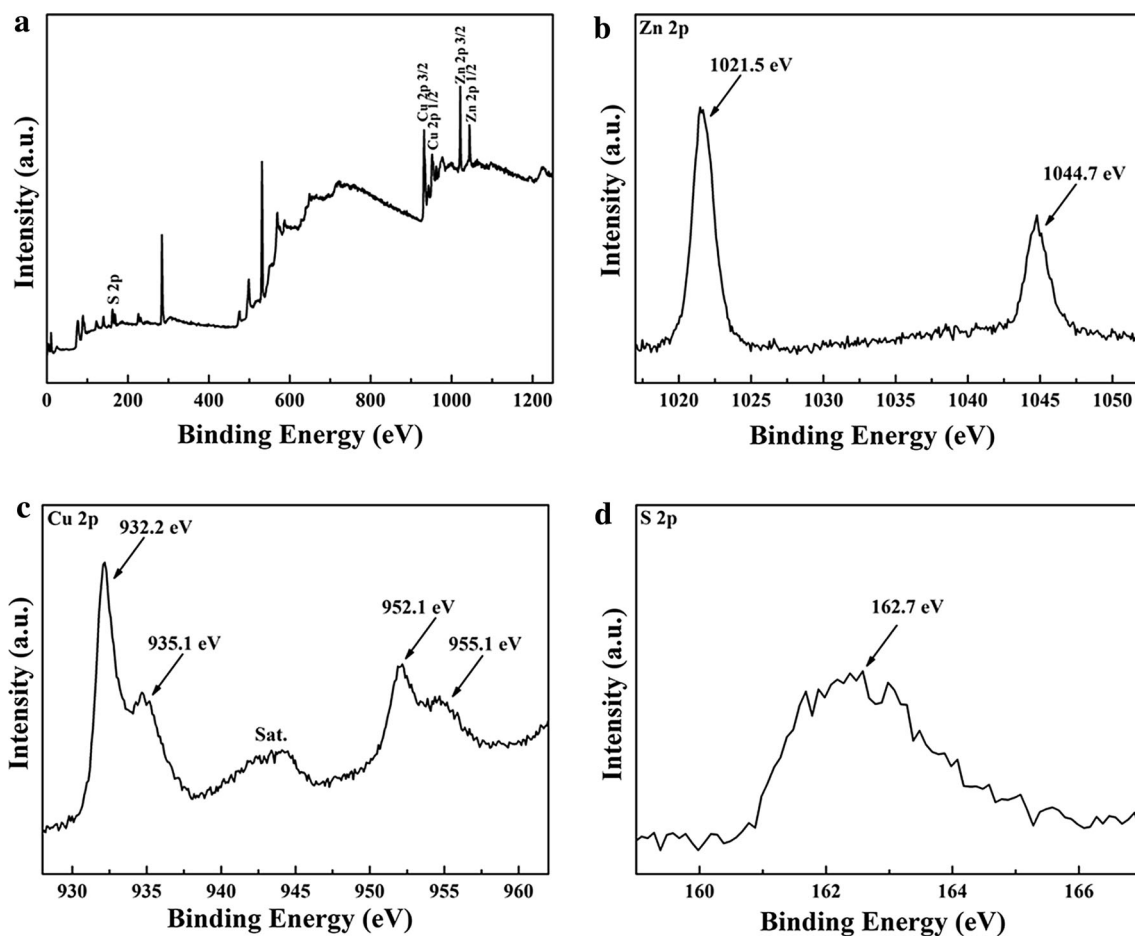

Fig. 4 The XPS of the CCNFs/ZnO/CuS nanocomposites **a** Full survey, **b** Zn 2p spectrum, **c** Cu 2p spectrum, **d** S 2p spectrum
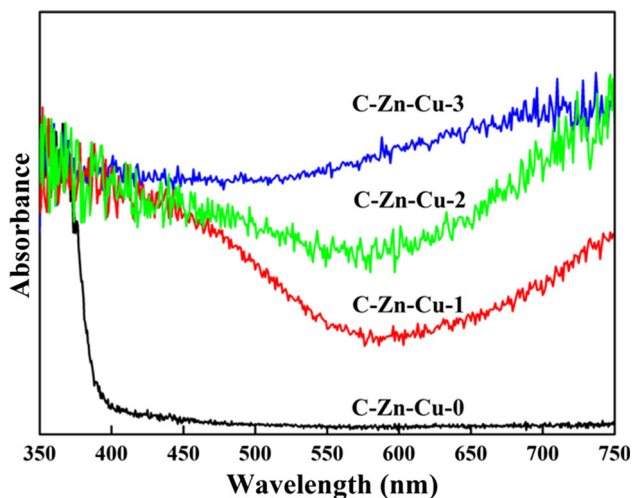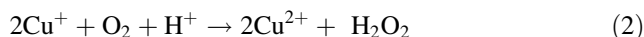
Fig. 5 UV–visible absorption spectra of the CCNFs/ZnO/CuS nanocomposites with different amount of CuS

also considered as one of the main reasons for the enhancement of visible light photocatalysis. What's more, the additional absorption in the range of 700–750 nm is due to the d–d transition of Cu^{2+} [29, 30].

As shown in Fig. 6a, the photocatalytic activity of the C–Zn–Cu-X composites is evaluated by the decomposition of MB under visible light. It is obviously that the pure CCNFs are deactivated under visible light. As seen, the CuS with weakly photocatalysis because of its feeblish dispersibility, and the CNNFs/ZnO also with weakly photocatalysis which caused by the surface defect of ZnO [9]. It is interesting that the nanocomposites(C–Zn–Cu-1, C–Zn–Cu-2, C–Zn–Cu-3) exhibit remarkable photocatalysis after CuS are introduced, as seen, the degradation increases with the CuS (~97.9%) until C–Zn–Cu-2, then decrease, which indicates that the suitable amount of CuS can effectively improve the visible light photocatalytic performance.

As a remarkable photocatalyst, it is interesting to investigate the recycling stability and retrievability of the C–Zn–Cu-2 under visible light. As shown in Fig. 6b, after nine consecutive recycle, the photocatalysis decrease less, which may bring an advantage to the photocatalyst for the promising practical application.

Based on the above result, it is significantly to investigate the role of CuS in the CCNF/ZnO/CuS nanocomposites. In this system, after CuS were introduced into the nanocomposites system, the direct interfacial charge transfer (IFCT) from the VB of ZnO to CuS could be considered as the main reason [22, 31, 32]. Under the visible light, electrons in the VB of semiconductors are directly transferred to Cu^{2+} and reduced to Cu^{+}, which plays an important role in charge separation and reducing recombination, then the produced Cu^{+} is converted back to Cu^{2+} when it reacts with adsorbed O_2 dissolved in the solution [33, 34]. So the proposed mechanism of the heterostructure could be described as follows [22, 35]:

$$2Cu^{2+} + 2e^{-} \rightarrow 2Cu^{+} \tag{1}$$

$$2Cu^{+} + O_2 + H^{+} \rightarrow 2Cu^{2+} + H_2O_2 \tag{2}$$

$$H_2O_2 \rightarrow 2 \cdot OH \tag{3}$$

What's more, as the presence of defect, the ZnO could response for part of visible light, as shown in Fig. 7, which is a typical process and could make the ubiquitously present molecular oxygen to form $\cdot O_2$ [9]. These two processes are considered as the main reasons for the visible light photocatalysis. In addition, Benefiting from the 3D-net structure, majority of photons remain within the branch structure until completely absorbed, which is also considered as a nonnegligible reason. At the same time, the branch structure could promote the CCNFs/ZnO/CuS nanocomposites dispersing in sewage to utilize the luminous energy more effectively. It is interesting that there is
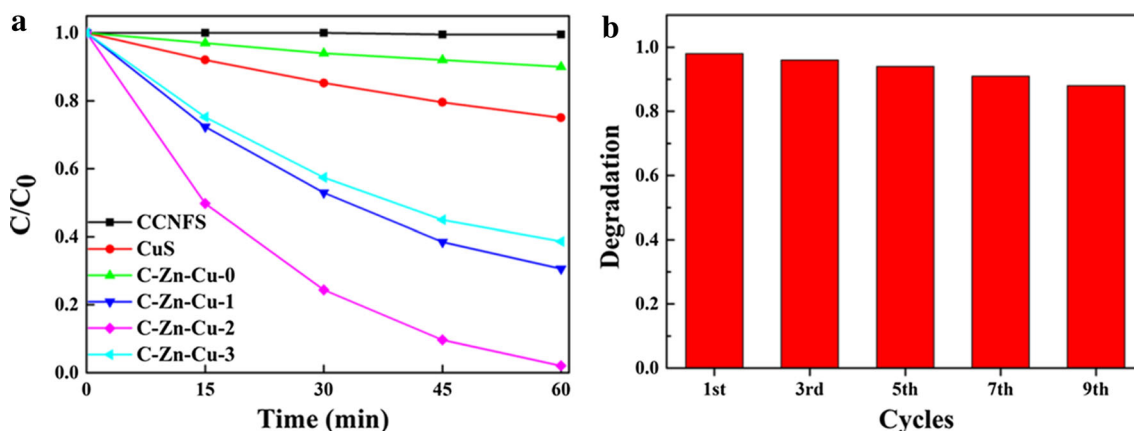

Fig. 6 a Photocatalytic degradation of MB solution by C–Zn–Cu-X composites with different amount of CuS under visible light irradiation, **b** recycle curve of C–Zn–Cu-2
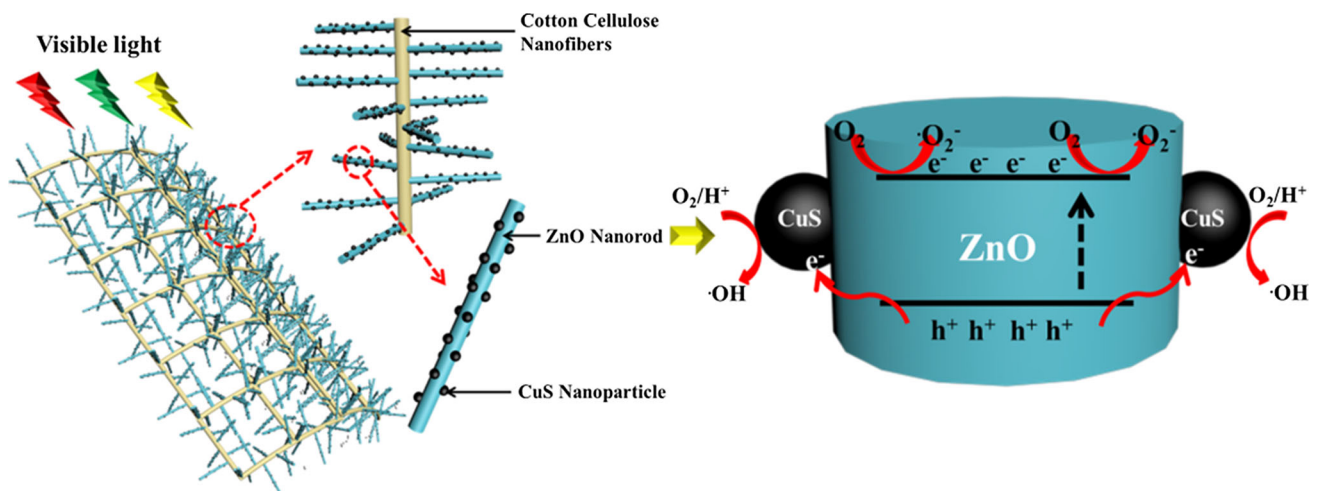
Fig. 7 schematic illustration of the photocatalytic process for CCNFs/ZnO/CuS composites under visible light

an obvious decrease with excess amount of CuS, which result from decreased active sites caused by superfluous CuS nanoparticles loaded on the surface.

In light of the above advantages, the 3D CCNFs/ZnO/CuS nanocomposites can efficiently degrade the MB solution and be expected to be a remarkable catalyst.

4 Conclusions

In summary, the CCNFs/ZnO/CuS nanocomposites prepared by a simple process and proved excellent visible light photocatalytic activity in MB degradation, which could be mainly attributed to the unique IFCT behaviour of the ZnO/CuS heterostructure and the defect in ZnO nanorods. In addition, the 3D net structure is also considered as an important reason for remarkable catalytic properties. Such recyclable composites may bring new insight to design the green and highly efficient catalyst in environmental pollution control and potential soft photoelectric technological applications.

References

1. E.J. Shin, S.M. Choi, D. Singh, S.M. Zo, Y.H. Lee, J.H. Kim, S.S. Han, Cellulose **21**, 3515 (2014)
2. T. Subbiah, G.S. Bhat, R.W. Tock, S. Parameswaran, S.S. Ramkumar, J. Appl. Polym. Sci. **96**, 557 (2005)
3. A. Frenot, I.S. Chronakis, Curr. Opin. Colloid Interface Sci. **8**, 64 (2003)
4. V.L. Pushparaj, M.M. Shaijumon, A. Kumar, S. Murugesan, L.J. Ci, R. Vajtai, R.J. Linhardt, O. Nalamasu, P.M. Ajayan, Proc. Natl. Acad. Sci. USA **104**, 13574 (2007)
5. L.B. Hu, H. Wu, F.L. Mantia, Y. Yang, Y. Cui, ACS Nano **4**, 5843 (2010)
6. D.H. Kim, Y.S. Kim, J. Wu, Z. Liu, J. Song, H.S. Kim, Y.Y. Huang, K.C. Hwang, J.A. Rogers, Adv. Mater. **21**, 3703 (2009)
7. K. Rodríguez, S. Renneckar, P. Gatenholm, ACS Appl. Mater. Interfaces **3**, 681 (2011)
8. C.R. Li, R. Chen, X.Q. Zhang, J. Xiong, Y.Y. Zheng, W.J. Dong, Fibers Polym. **12**, 345 (2011)
9. X. Zhang, J.Q. Pan, C.Q. Zhu, Y.Z. Sheng, Z.X. Yan, Y.M. Wang, B.X. Feng, J. Mater. Sci.: Mater. Electron. **26**, 2861 (2015)
10. X.J. Yu, J.J. Liu, Y.C. Yu, S.L. Zuo, B.S. Li, Carbon **68**, 718 (2014)
11. K.M. Lee, C.W. Lai, K.S. Ngai, J.C. Juan, Water Res. **88**, 428 (2016)
12. C.G. Tian, Q. Zhang, A.P. Wu, M.J. Jiang, Z.L. Liang, B.J. Jiang, H.G. Fu, Chem. Commun. **48**, 2858 (2012)
13. A.S. Jamal, B. Tanujjal, A.A. Mohammed, D. Joydeep, Materials **9**, 238 (2016)
14. J.Q. Yuan, E.S.G. Choo, X.S. Tang, Y. Sheng, J. Ding, J.M. Xue, Nanotechnology **21**, 185606 (2010)
15. H. Yamada, Y. Ushimi, M. Takeuchi, Y. Yoshino, T. Makino, S. Arai, Vacuum **74**, 689 (2004)
16. P. Li, Z. Wei, T. Wu, Q. Peng, Y.D. Li, J. Am. Chem. Soc. **133**, 5660 (2011)
17. Q. Wang, B.Y. Geng, S.Z. Wang, Environ. Sci. Technol. **43**, 8968 (2009)
18. C.L. Ren, B.F. Yang, M. Wu, J. Xu, Z.P. Fu, Y. Lv, T. Guo, Y.X. Zhao, C.Q. Zhu, J. Hazard. Mater. **182**, 123 (2010)
19. G.M. Wang, X.Y. Yang, F. Qian, J.Z. Zhang, Y. Li, Nano Lett. **10**, 1088 (2010)
20. X.W. Wang, G. Liu, G.Q. Lu, H.M. Cheng, Int. J. Hydrogen Energy **35**, 8199 (2010)
21. B. GaoJ, J.M. Luther, O.E. Semonin, R.J. Ellingson, A.J. Nozik, M.C. Beard, Nano Lett. **11**, 1002 (2011)
22. M. Lee, K. Yong, Nanotechnology **23**, 194014 (2012)
23. L.J. Zhang, T.F. Xie, D.J. Wang, S. Li, L.L. Wang, L.P. Chen, Y.C. Lu, Int. J. Hydrogen Energy **38**, 11811 (2013)
24. P. Gomathisankar, K. Hachisuka, H. Katsumata, T. Suzuki, K. Funasaka, S. Kaneco, Int. J. Hydrogen Energy **38**, 8625 (2013)
25. S. Khanchandani, S. Kumar, A.K. Ganguli, ACS Sustain. Chem. Eng. **4**, 1487 (2016)
26. C. Lu, C.Z. Liu, R. Chen, X.X. Fang, K. Xu, D.W. Meng, J Mater. Sci.: Mater. Electron. **27**, 6947 (2016)
27. Y. Im, S. Kang, K.K. Kim, T. Ju, G.B. Han, N.K. Park, T.J. Lee, M. Kang, Int. J. Photoenergy **2013**, 452542 (2013)

28. S. Li, Z.H. Ge, B.P. Zhang, Y. Yao, H.C. Wang, J. Yang, Y. Li, C. Gao, Y.H. Lin, Appl. Surf. Sci. **384**, 272 (2016)
29. X. Qiu, M. Miyauchi, H. Yu, H. Irie, K. Hashimoto, J. Am. Chem. Soc. **132**, 15259 (2010)
30. H. Irie, S. Miura, K. Kamiya, K. Hashimoto, Chem. Phys. Lett. **457**, 202 (2008)
31. H. Irie, K. Kamiya, T. Shibanuma, S. Miura, D.A. Tryk, T. Yokoyama, K. Hashimoto, J. Phys. Chem. C **113**, 10761 (2009)
32. Y.X. Zhao, H.C. Pan, Y.B. Lou, X.F. Qiu, J.J. Zhu, C. Burda, J. Am. Chem. Soc. **131**, 4253 (2009)
33. N. Kitajima, Y. Moro-oka, Chem. Rev. **94**, 737 (1994)
34. F. Himo, L.A. Eriksson, F. Maseras, P.E.M. Siegbahn, J. Am. Chem. Soc. **122**, 8031 (2000)
35. A.P. Cole, D.E. Root, P. Mukherjee, E.I. Solomon, T.D.P. Stack, Science **273**, 1848 (1996)